

Hubble's Imaging Surveys of the Ultraviolet universe: Panchromatic Extragalactic Research

Rogier Windhorst (Arizona State University) & the ERS UV team
and Harry I. Teplitz (IPAC, Caltech; PI of the UV-UDF team)

& T. Ashcraft, H. Atek, N. Bond, T. Brown, G. Bruzual, D. Calzetti, S. Casertano, D. Coe, S. Cohen, J. Colbert, C. Conselice, Y. Dai, D. de Mello, M. Dickinson, S. Driver, H. Ferguson, K. Finkelstein, S. Finkelstein, J. Frogel, J. Gallego, J. Gardner, E. Gawiser, M. Giavalisco, A. Grazian, N. Grogin, C. Gronwall, D. Hanish, N. Hathi, T. Heckman, R. Jansen, C. Kaleida, S. Kassin, S. Kaviraj, H. Kim, A. Koekemoer, D. Koo, P. Kurczynski, K.-S. Lee, Z. Levay, J. Lotz, R. Lucas, J. MacKenty, S. Malhotra, P. McCarthy, M. Mechtley, G. Meurer, M. Mutchler, K. Noeske, R. O'Connell, R. Overzier, N. Pirzkal, M. Rafelski, S. Ravindranath, J. Rhoads, M. Rieke, B. Robertson, M. Rutkowski, R. Ryan, C. Scarlata, M. Seibert, S. Salim, B. Siana, J. Silk, E. Soto, A. Straughn, K. Tamura, E. Voyer, S. Wilkins, H. Yan, & S. Yi

Presentation to Science Analysis Group #7, NASA Cosmic Origins Program Analysis Group (COPAG).

Monday June 2, 2014, 10:30–11:30 am; 224st AAS meeting, Westin Copley Place, Boston, MA.

Outline and 4 Science Goals

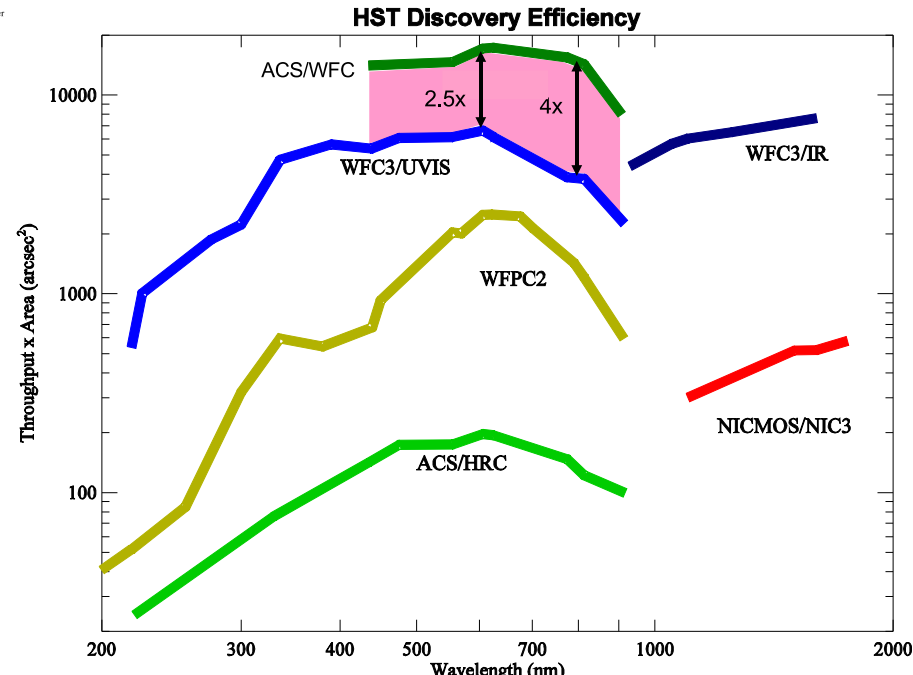
- Deep wide-field HST WFC3 UV imaging is critical NOW to prepare for JWST ($\lambda \gtrsim 0.7\mu\text{m}$), and to define a $\gtrsim 8$ -meter UV-optical sequel to HST:
- (1) The physics and evolution of SF in low-mass galaxies over the LAST 9 Gyrs: Critical benchmark to understand cosmic reionization at $z \gtrsim 6$;
- (2) Evolution of the star/dust/gas mixture in SF regions, and the influence of supernovae and AGN feedback;
- (3) Evolution of young, star-forming sub-galactic clumps induced by mergers or gas accretion, and the growth of stable galaxy disks;
- (4) Late-epoch SF & structural evolution in massive early-type galaxies.
- (5) Summary and Conclusions.



Goddard Space Flight Center

Hubble Space Telescope Program

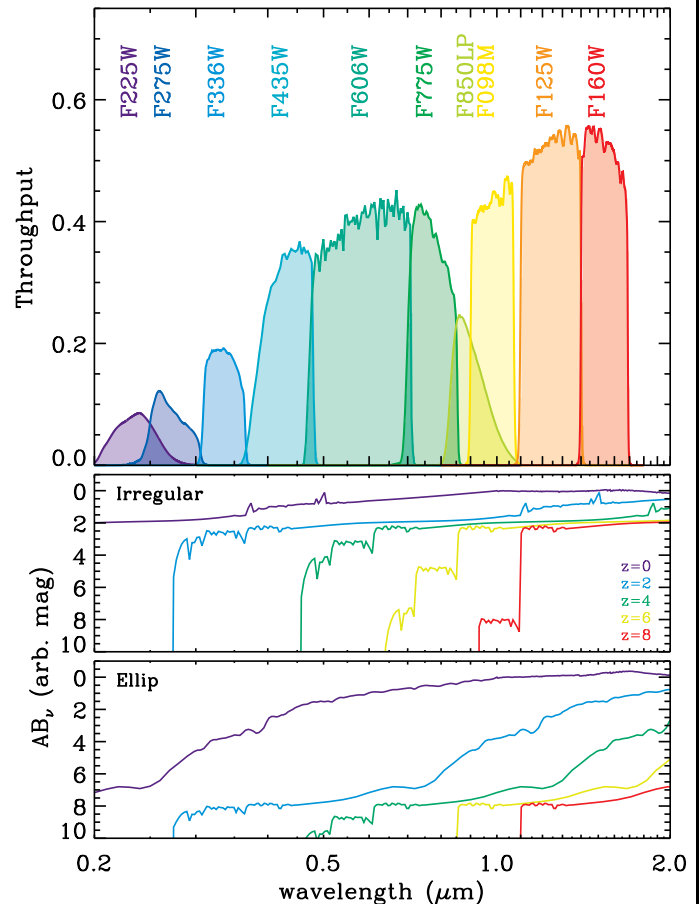
Role of ACS in HST Post-SM4 Imaging Capability



ACS/WFC superior to WFC3 survey efficiency at visible-red wavelengths

030507_PMB_ACSS_Status.ppt

9



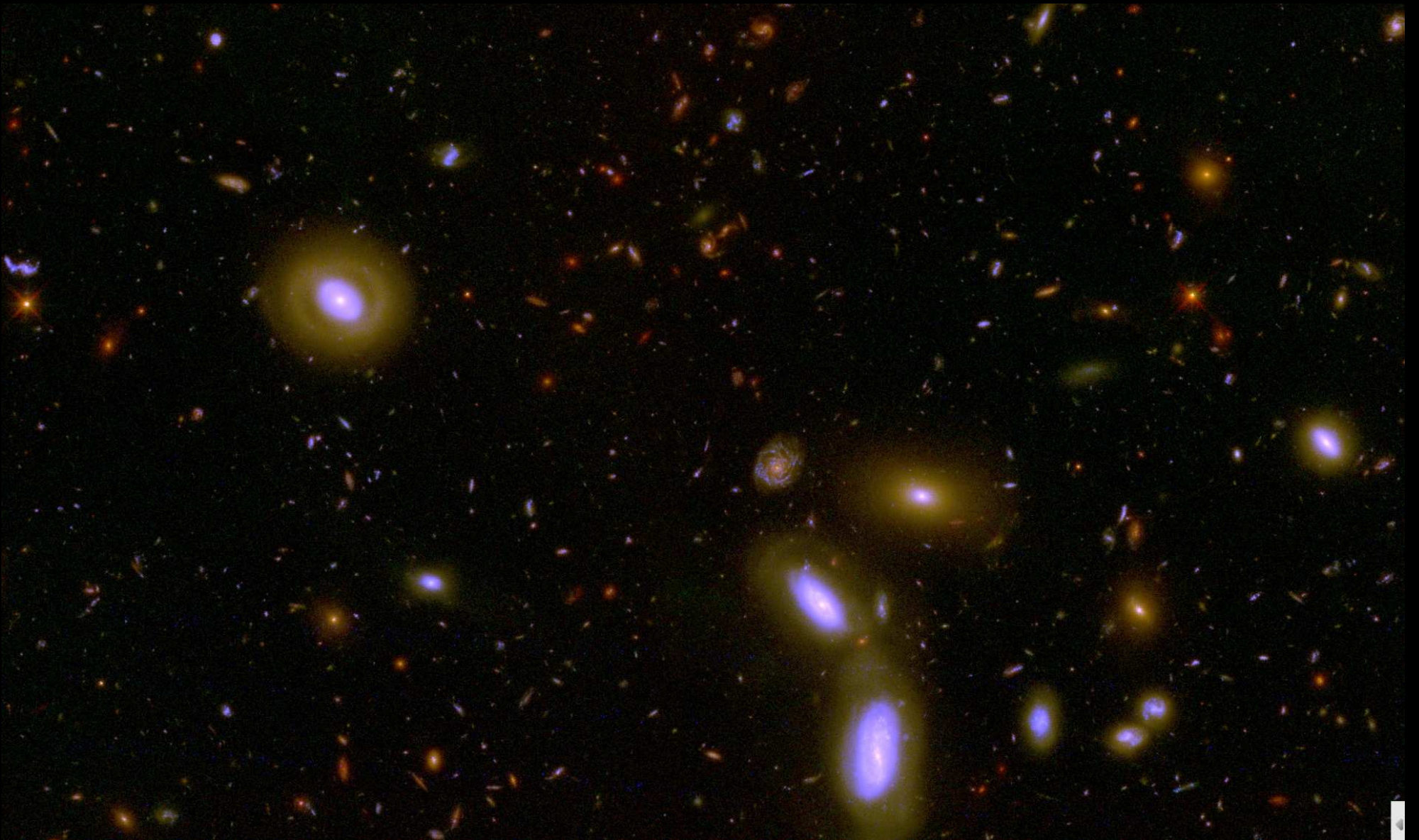
WFC3/UVIS channel unprecedented UV–blue throughput & areal coverage:

$\text{QE} \gtrsim 70\%$, $4k \times 4k$ array of $0\farcs04$ pixel, $\text{FOV} \simeq 2\farcm67 \times 2\farcm67$.

WFC3/IR channel unprecedented near-IR throughput & areal coverage:

$\text{QE} \gtrsim 70\%$, $1k \times 1k$ array of $0\farcs13$ pixel, $\text{FOV} \simeq 2\farcm25 \times 2\farcm25$.

- WFC3 filters designed for star-formation and galaxy assembly at $z \simeq 0\text{--}8$.
- HST WFC3 and its UVIS channel a critical pathfinder for JWST science.

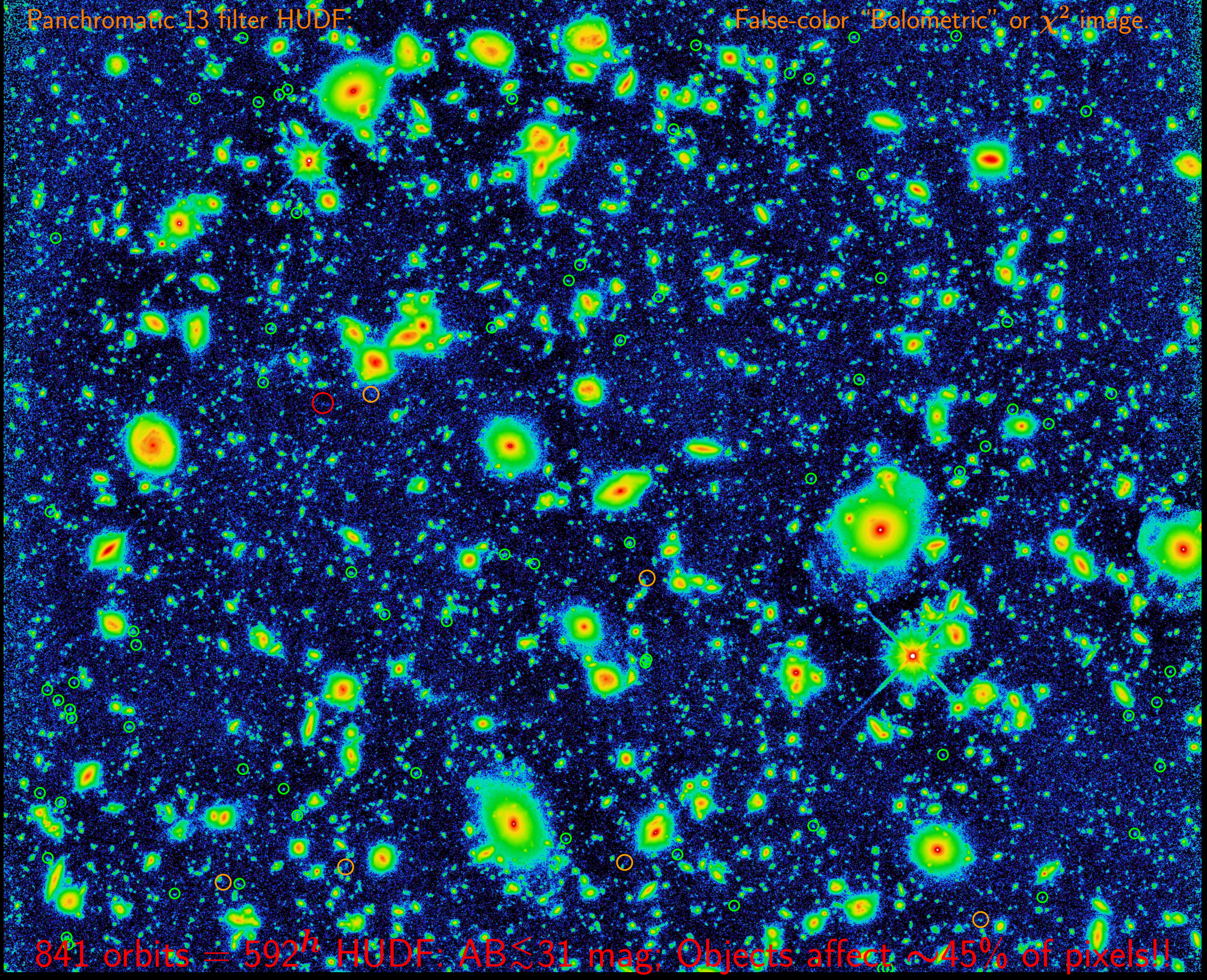


10 filters with HST/WFC3 & ACS reaching AB=26.5–27.0 mag (10σ) over 40 arcmin 2 at 0.07–0.15" FWHM from 0.2–1.7 μ m (UVUBVizYJH).

- ERS in GOODS-S v2: using WFC3 for what it was designed to do.
- JWST adds 0.05–0.2" FWHM imaging to AB \simeq 31.5 mag at 0.7–5 μ m, and 0.2–1.2" FWHM at 5–29 μ m, tracing young+old SEDs & dust.

Panchromatic 13 filter HUDF

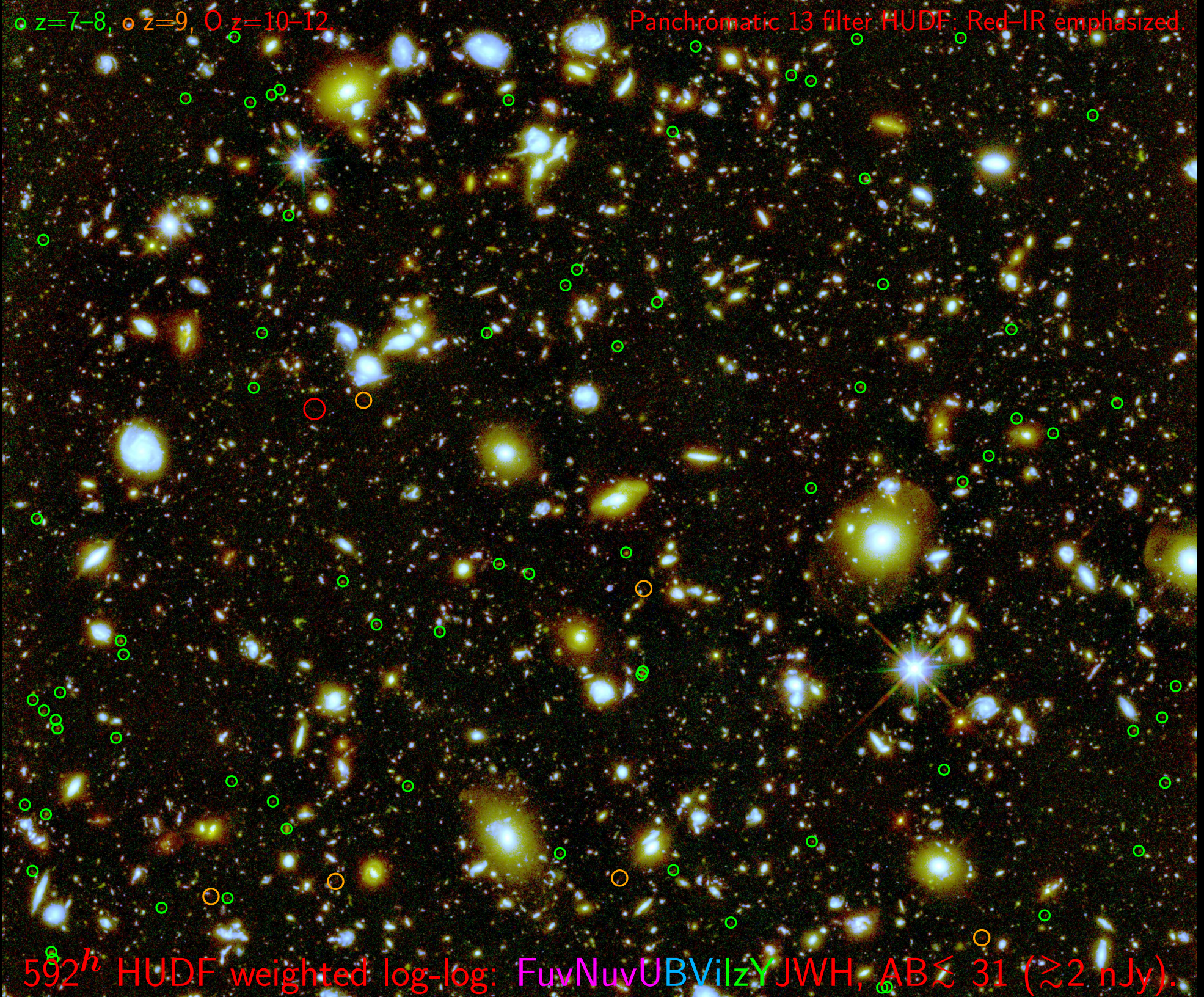
False-color "Bolometric" or χ^2 image.



841 orbits = 592^h HUDF: AB \lesssim 31 mag; Objects affect \sim 45% of pixels!!

○ $z=7-8$, ○ $z=9$, ○ $z=10-12$.

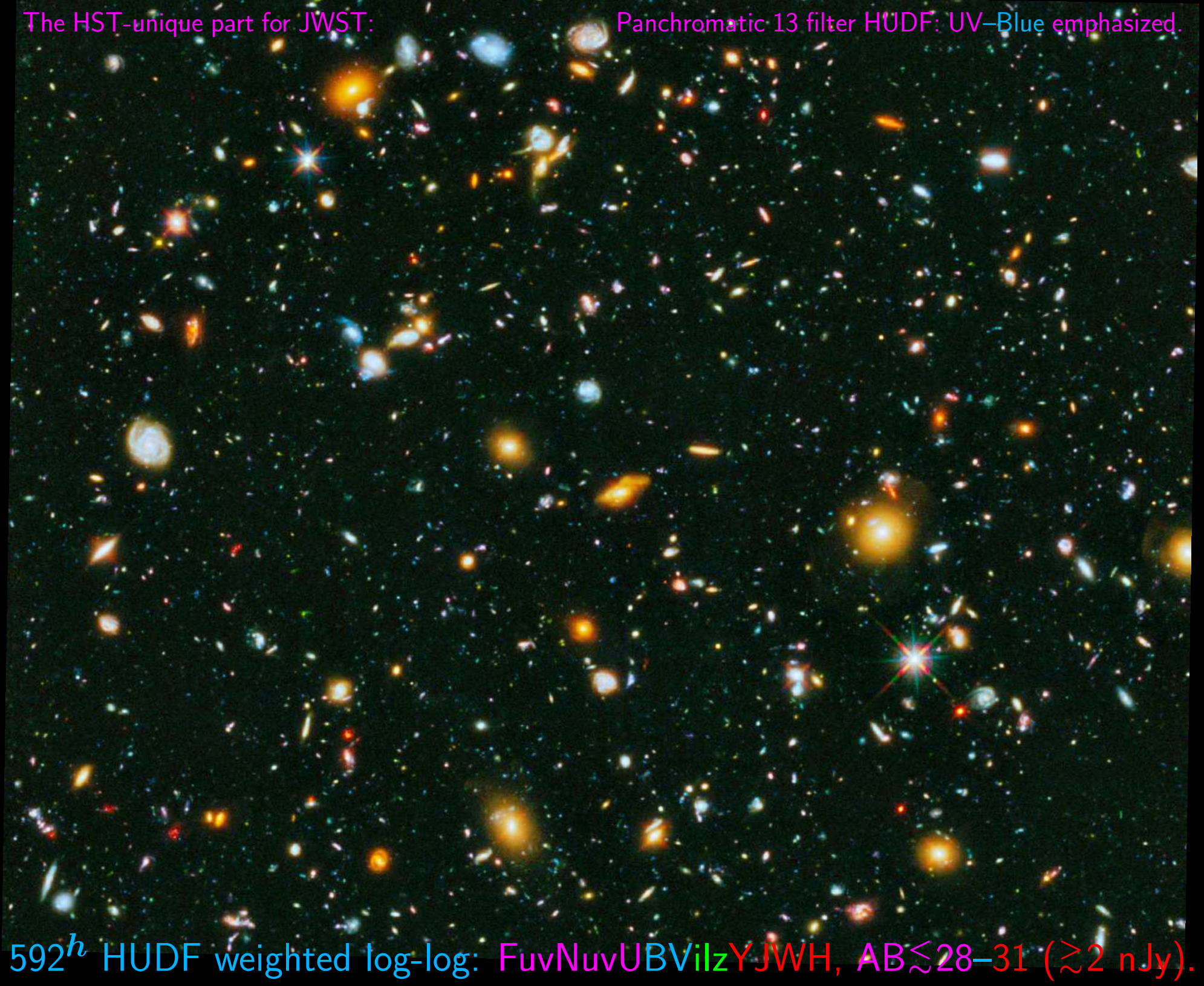
Panchromatic 13 filter HUDF; Red-IR emphasized.



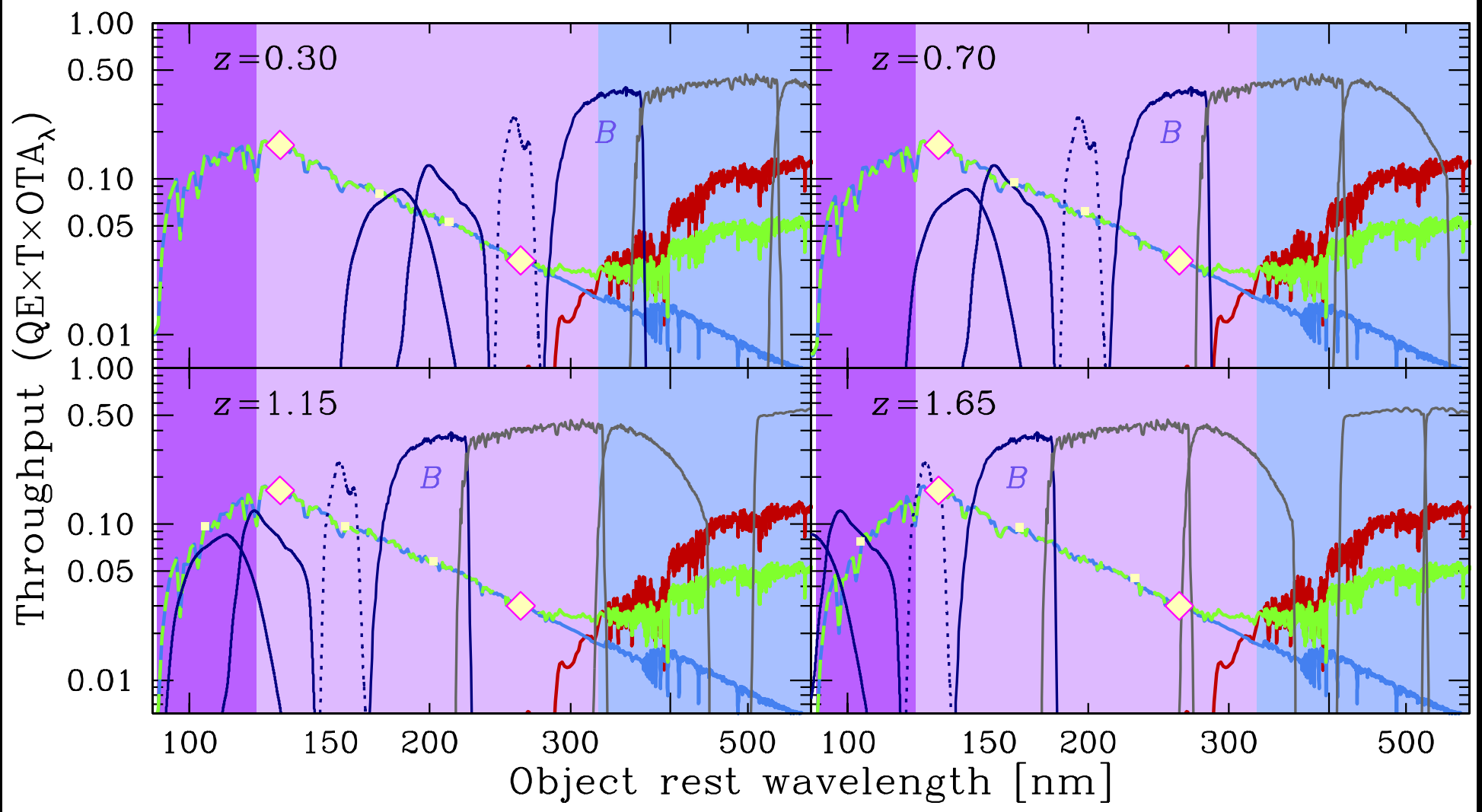
592^h HUDF weighted log-log: F_{UV}N_{UV}U_{BV}I_{zYJWH}, AB $\lesssim 31$ ($\gtrsim 2$ nJy).

The HST-unique part for JWST:

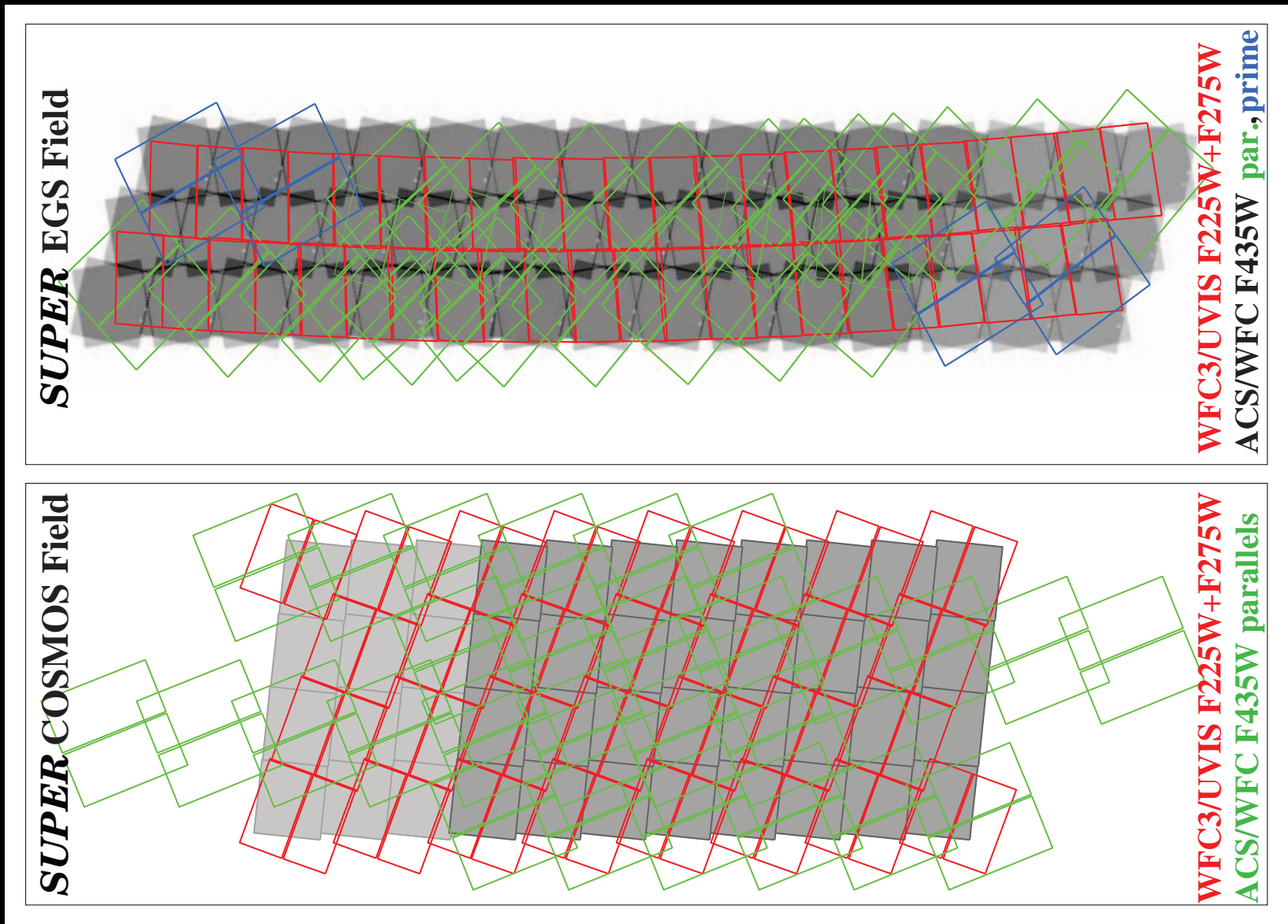
Panchromatic 13 filter HUDF: UV-Blue emphasized.



592^h HUDF weighted log-log: FuvNuvUBViIzYJWH, AB<28-31 ($\gtrsim 2$ nJy).

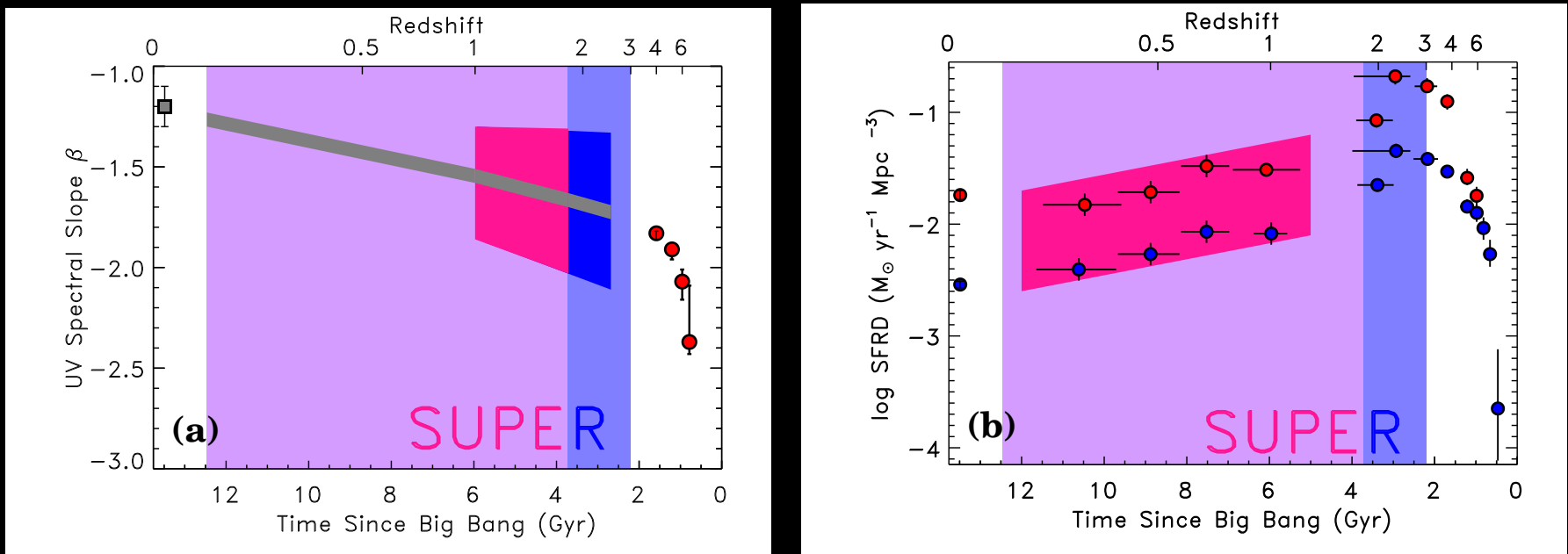


- Rest-frame SEDs of objects with young, mixed, and old stellar populations with WFC3 UV, ACS B & CANDELS VIJH filters.
- Diamonds: Rest-frame 1300Å and 2600Å to measure UV β -slope.
- For $0.2 \lesssim z \lesssim 2.0$ WFC3 UV, ACS F435W & CANDELS (F606W, F814W) filters sample the β -slope for SF objects in $\gtrsim 2$ filters at $\lesssim 0''.1$ FWHM.



- Viable APT solutions to cover CANDELS fields (split over 2 ORIENTs ~180 days apart to aid scheduling).
- WFC3/UVIS tiles in red, ACS/F435W tiles in green (parallels), or blue (primary); CANDELS WFC3/IR F125W, F160W tiles in grey.

(1) Physics and evolution of SF in low-mass galaxies over the LAST 9 Gyrs:

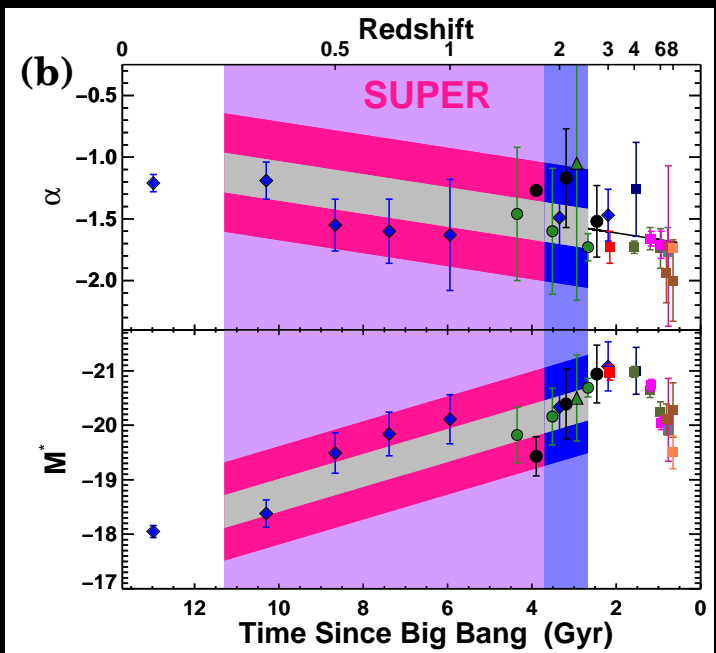
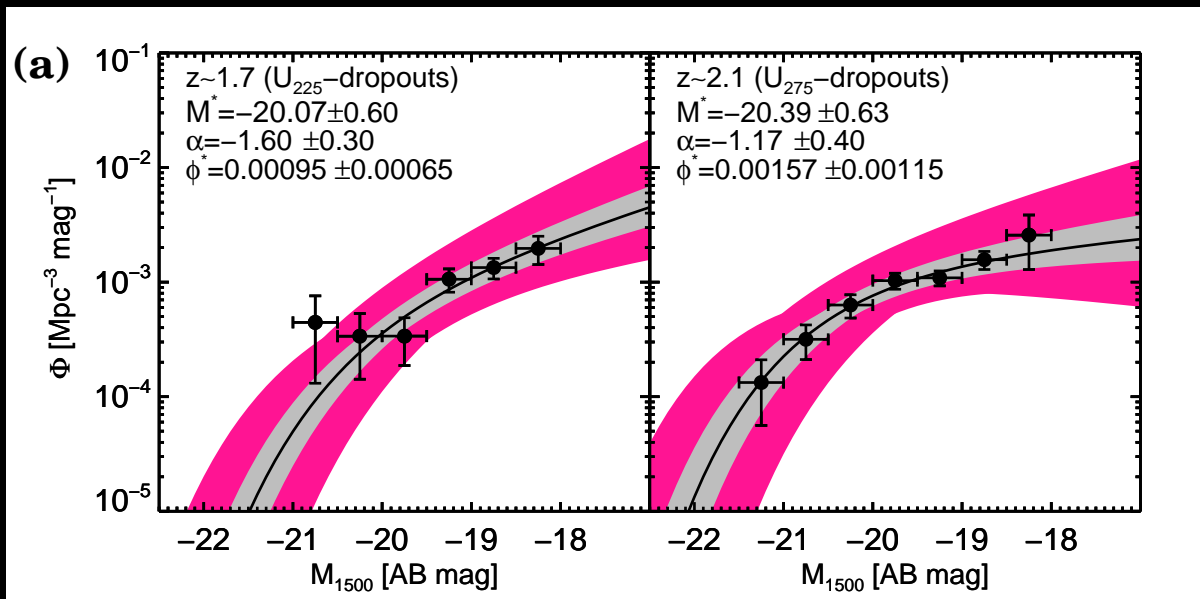


[LEFT] Evolution of the UV spectral slope β (Finkelstein et al. 2011). Dark pink/dark blue region is WFC3 ERS β -range (Hathi et al. 2012).

- Deep wide-field WFC3 UV traces β -evolution for 16,000 SF clumps at $0.2 \lesssim z \lesssim 2$ (grey strip) \Rightarrow dust A_V in SF knots of sub- L^* galaxies.

[RIGHT] Evolution of the cosmic SF-rate density (“SFRD”; Bouwens et al. 2011). Blue dots are before and red dots after dust-correction.

- Deep wide-field WFC3 UV will yield SFRD in low-mass galaxies at $z \lesssim 2$.
- Essential synergy with Herschel FIR \Rightarrow relation between β and dust attenuation, providing the most robust estimate of the SFRD at $z \lesssim 2$.

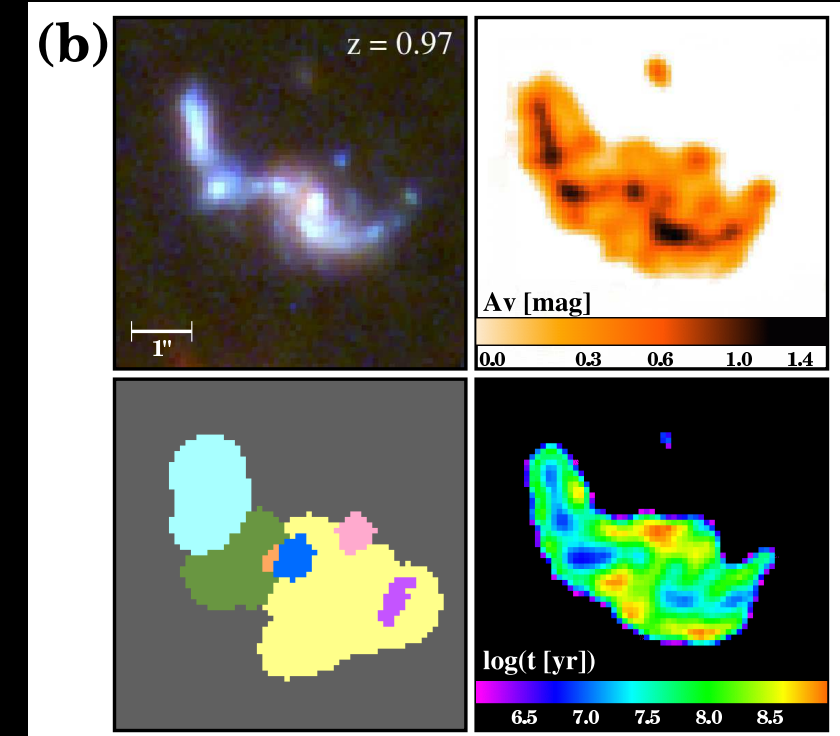
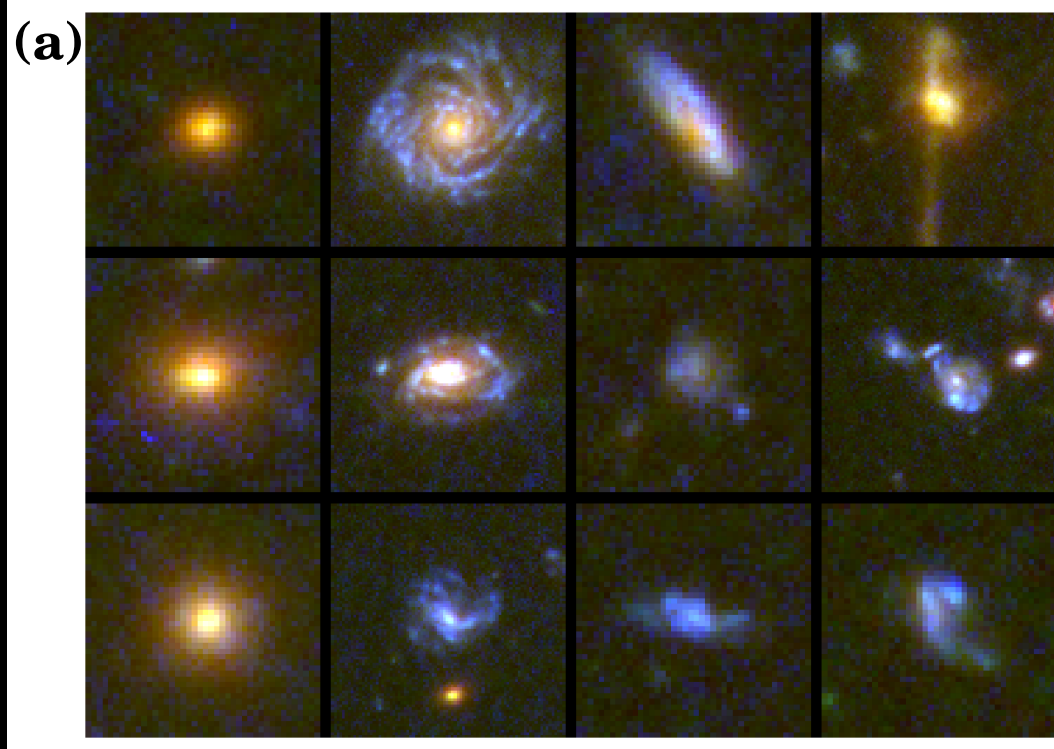


[LEFT panels] Rest-frame UV Luminosity Functions (LFs) based on UV-dropouts (Hathi et al. 2010, 2012).

[RIGHT] ● (top) Evolution of the faint-end Schechter slope α and M^* (e.g., Hathi et al. 2010, Oesch et al. 2010b).

● (Bottom) M^* vs. z behavior resembles the cosmic SF history (Madau et al. 1996), and reflects the process of galaxy assembly and downsizing.

- Dark pink indicates current WFC ERS + CANDELS uncertainties.
- Grey wedge shows the significant improvement from deep wide-field WFC3 UV imaging for $0.2 \lesssim z \lesssim 2.5$.

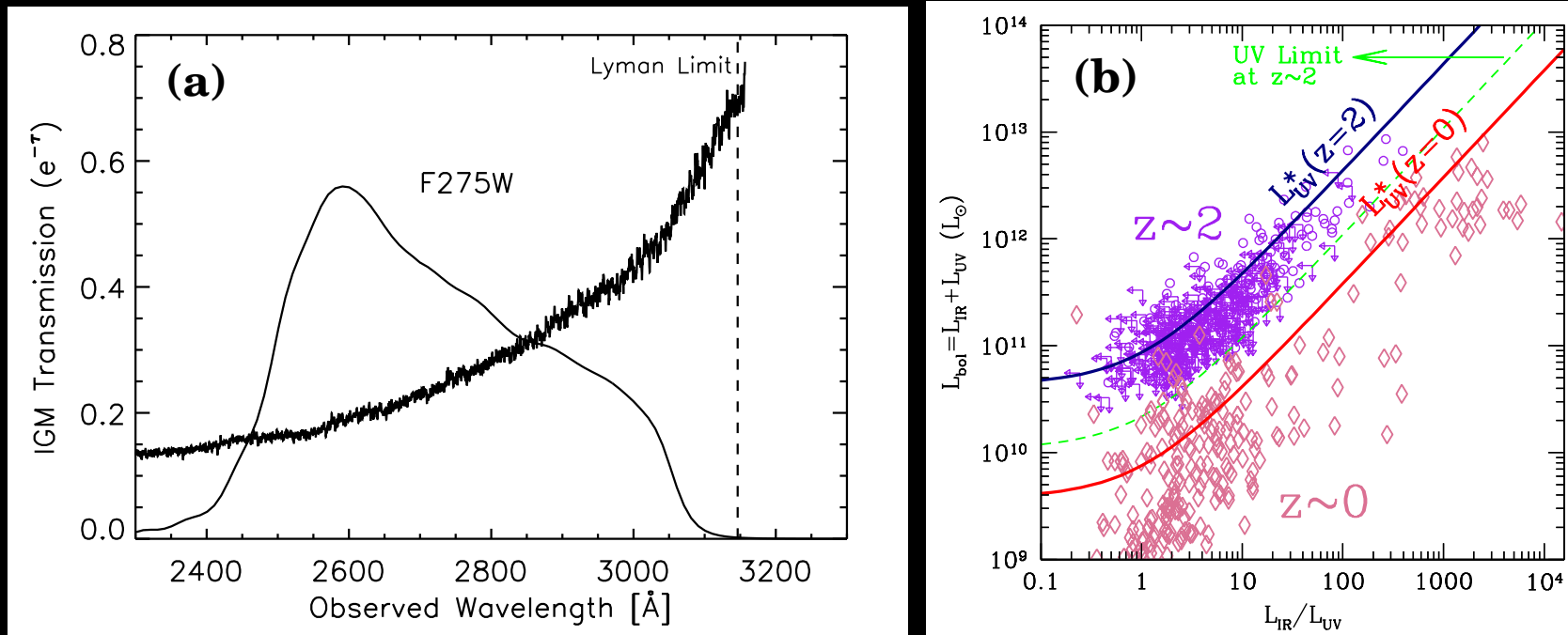


[LEFT panels] WFC3 ERS color images of galaxies at $z \approx 0.75$ shown in the 7 WFC3 UV+B & CANDELS filters. All show measurable UV flux.

[RIGHT] $z \approx 1$ galaxy in same filters (upper left). WFC3 UV priors can dissect deep ground-based U₃₆₀-images ($0\farcs9$ FWHM; Grazian et al. 2006), recovering fluxes for $\gtrsim 65\%$ of HST's SF-clumps (lower left).

- Right panels show pixel-to-pixel dust (A_V) & SF-age ($\log t/\text{yr}$) maps.
- Deep wide-field WFC3 UV will yield pixel-to-pixel mass, age, A_V and dust-maps for ~ 2000 galaxies at $0.2 \lesssim z \lesssim 2$.

(2) Evolution of star/dust/gas mix in SF regions, and SNe/AGN feedback:



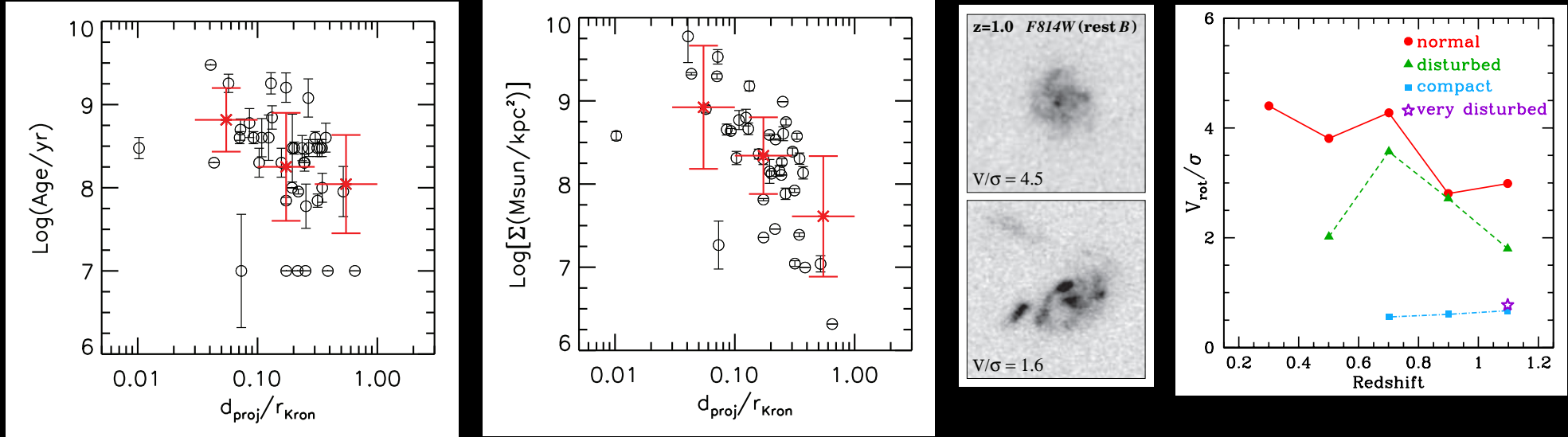
[LEFT] Average IGM transmission vs. wavelength. WFC3 F275W samples Lyman-continuum escape fraction f_{esc} at $z \approx 2.45$, where average transmission is $e^{-\tau} \approx 0.250$ (Siana et al. 2012).

- Deep wide-field WFC3 UV will yield f_{esc} for ~ 800 galaxies at $z \approx 2.45$, and relate it to physical galaxy properties (mass, type, A_V , V_{rot}/σ_g).

[RIGHT] Bolometric luminosity vs. dust attenuation ($L_{\text{IR}} / L_{\text{UV}}$) for $z \approx 2$ compared to local galaxies (Reddy et al. 2010), suggesting evolution of the net extinction in SF galaxies with time.

- Deep wide-field WFC3 UV: +800 dusty LBGs in redshift gap $0.2 \lesssim z \lesssim 2$.

(3) Evolution of SF clumps and the growth of stable galaxy disks:



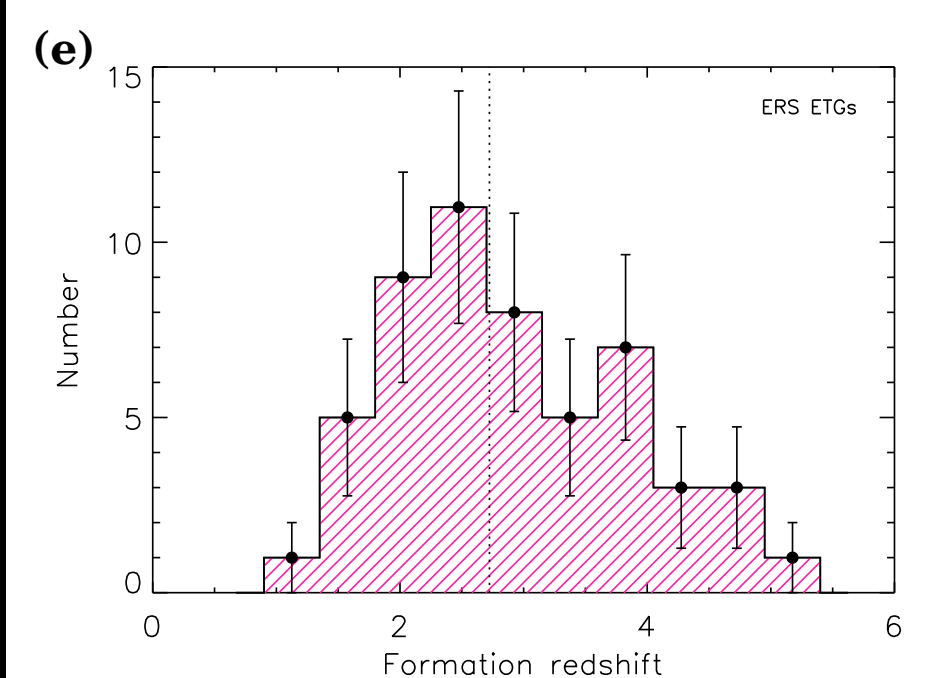
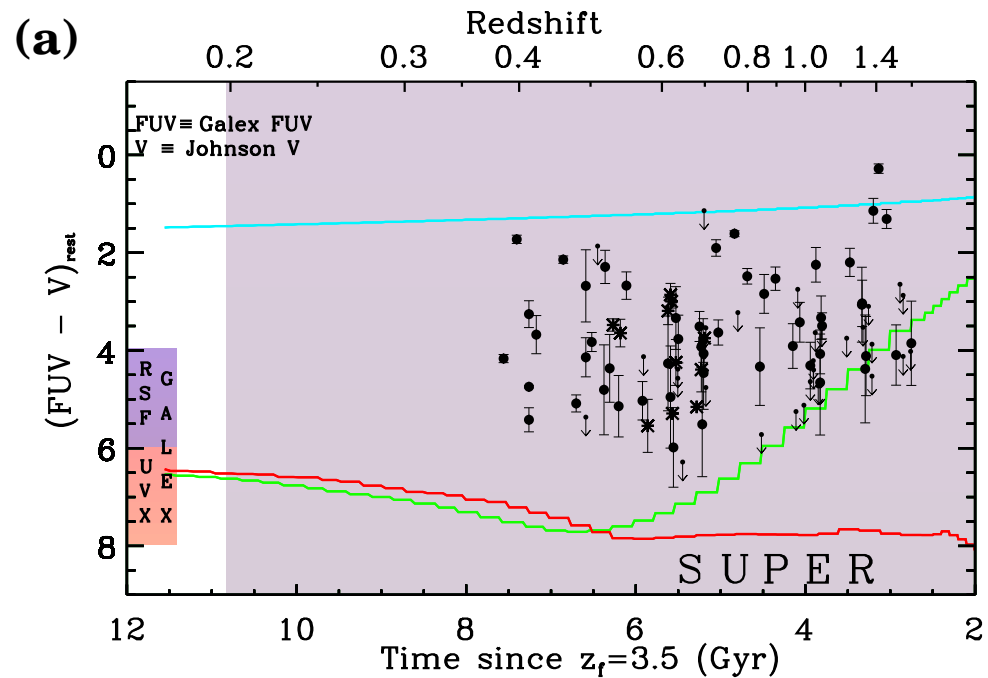
[LEFT 2 panels] Radial variation of age and mass surface-density of sub-galactic clumps at $z \approx 2$ vs. galacto-centric distance (Guo et al. 2011, 2012).

[MIDDLE 2] Ordered rotation (V_{rot}) & disturbed motions (σ_g) shows strong correlation with rest-frame blue morphology (Kassin⁺ 2007).

[RIGHT] Ratio of ordered/disordered motions (V_{rot}/σ_g) correlated with HST rest-frame *B*-band morphology: the most disturbed galaxies have the lowest V_{rot}/σ_g ratio (Kassin et al. 2007, 2012).

- Deep wide-Field WFC3 UV will yield $\lesssim 2000$ UV objects, showing how galaxies disks have grown and stabilized for $0.2 \lesssim z \lesssim 2$.

(4) Late-epoch SF and structural evolution in massive early-type galaxies.



- 10-band WFC3 ERS data measured rest-frame UV-light in nearly all early-type galaxies at $0.3 \lesssim z \lesssim 1.5$ (Rutkowski et al. 2012, ApJS, 199, 4).
- ⇒ Most ETGs have continued residual star-formation after they form.
- Can determine their $N(z_{form})$, which resembles the cosmic SFH diagram (Madau et al. 1996), directly constraining the process of galaxy assembly & down-sizing (Kaviraj et al. 2012, MNRAS).
- Deep wide-field WFC3 UV increases sample 10-fold, providing critical UV data to delineate the range in z_{form} for ETGs as function of mass.

(5) Conclusions

For as long as we still have HST, deep wide-field WFC3 UV surveys must be done to address the following critical science questions:

These are critical and unique data in preparation for JWST ($\lambda \gtrsim 0.7\mu\text{m}$), and to define a $\gtrsim 8$ -meter UV-optical sequel to HST:

- (1) The physics and evolution of SF in low-mass galaxies over the LAST 9 Gyrs: critical benchmark to understand cosmic reionization at $z \gtrsim 6$;
- (2) Evolution of the star/dust/gas mixture in SF regions, and the influence of supernovae and AGN feedback;
- (3) Evolution of young, star-forming sub-galactic clumps induced by mergers or gas accretion, and the growth of stable galaxy disks;
- (4) Late-epoch SF and structural evolution in massive early-type galaxies.

SPARE CHARTS

- References and other sources of material shown:

<http://www.asu.edu/clas/hst/www/jwst/> [Talk, Movie, Java-tool]

<http://www.jwst.nasa.gov/> & <http://www.stsci.edu/jwst/>

Bouwens, R. et al. 2010, ApJ, 709, L133

Bouwens, R. et al. 2011, ApJ, 737, 90

Finkelstein, S. et al. 2012, ApJ, 428, 925

Grazian, A., et al. 2006, A&A, 449, 951

Gardner, J. P., et al. 2006, Space Science Reviews, 123, 485

Guo, et al. 2011, ApJ, 735, 18

Hathi, N., et al. 2010, ApJ, 720, 1708

Kassin, S., et al. 2007, ApJ, 660, L35

Kaviraj, et al. 2012, MNRAS, 428, 925

Reddy, N., et al. 2010, ApJ, 712, 1070

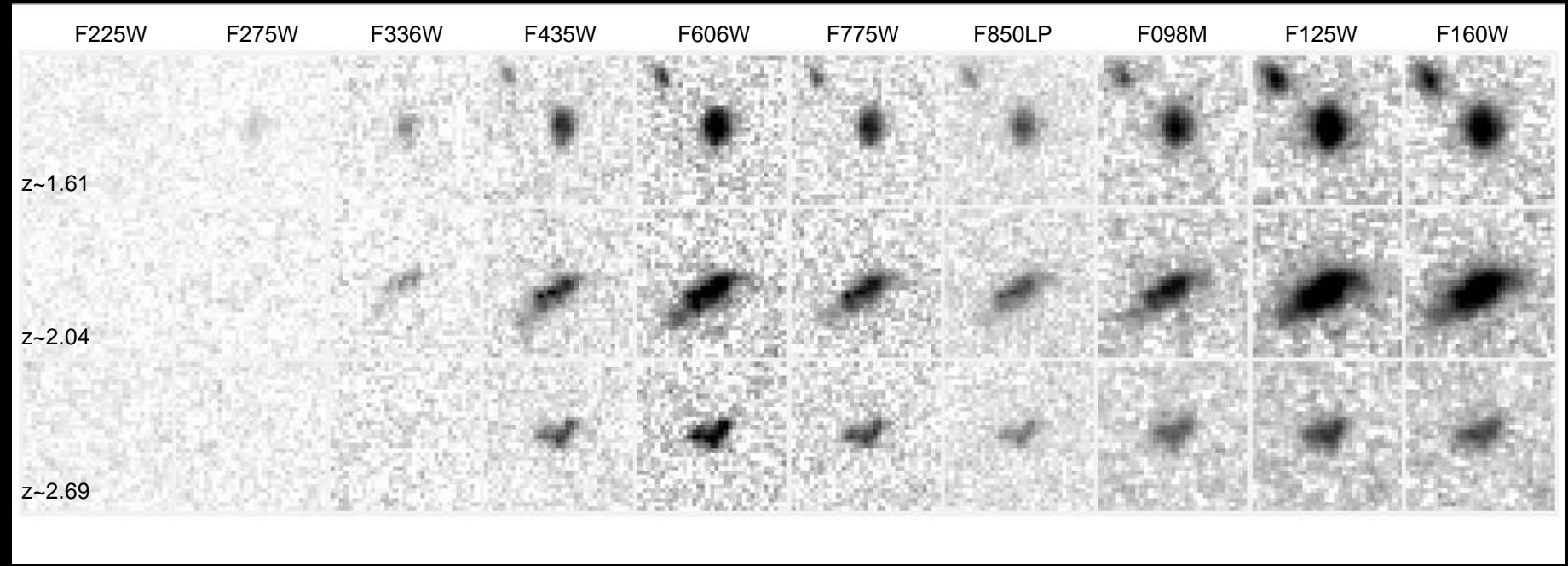
Rutkowski, et al. 2012, ApJS, 199, 4

Ryan, R., et al. 2012, ApJ, 749, 53

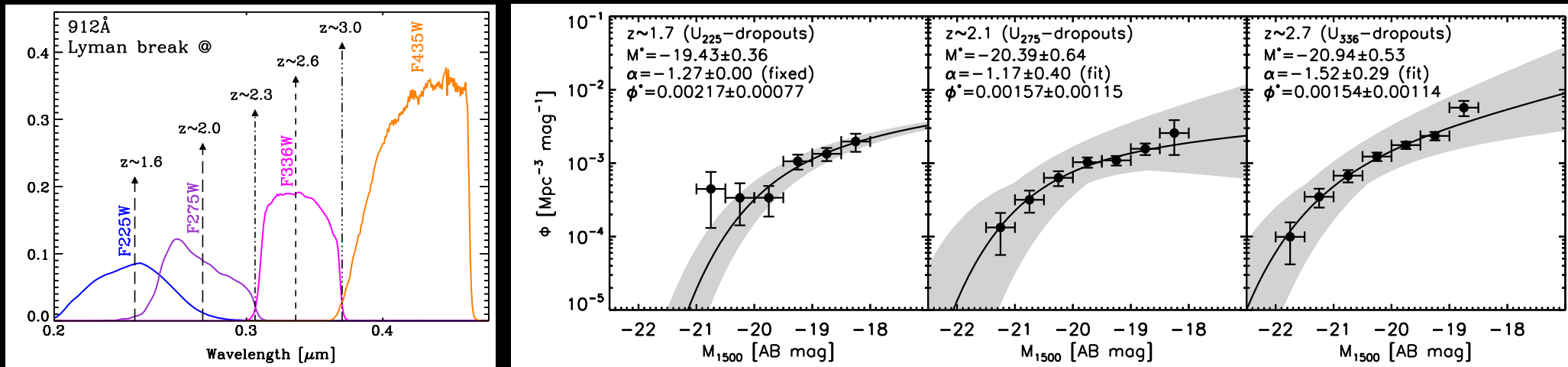
Siana, B., et al. 2010, ApJ, 723, 241

Teplitz, H. I., et al. 2013, AJ, 146, 159 & BAAS 224, 417.06 (this mtg)

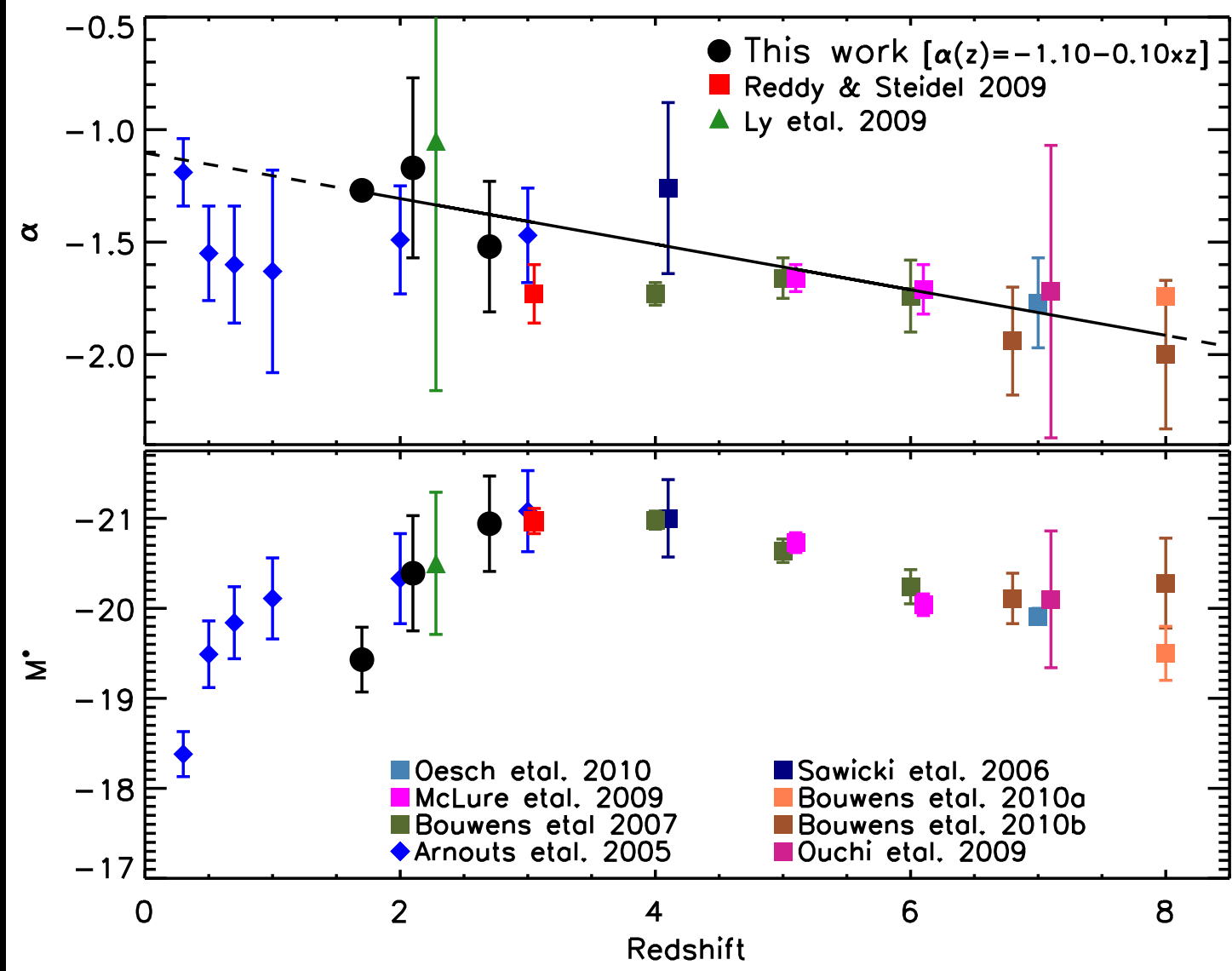
Windhorst, R., et al., 2011, ApJS, 193, 27



Lyman break galaxies at the peak of cosmic SF ($z \approx 1-3$; Hathi et al. 2010)

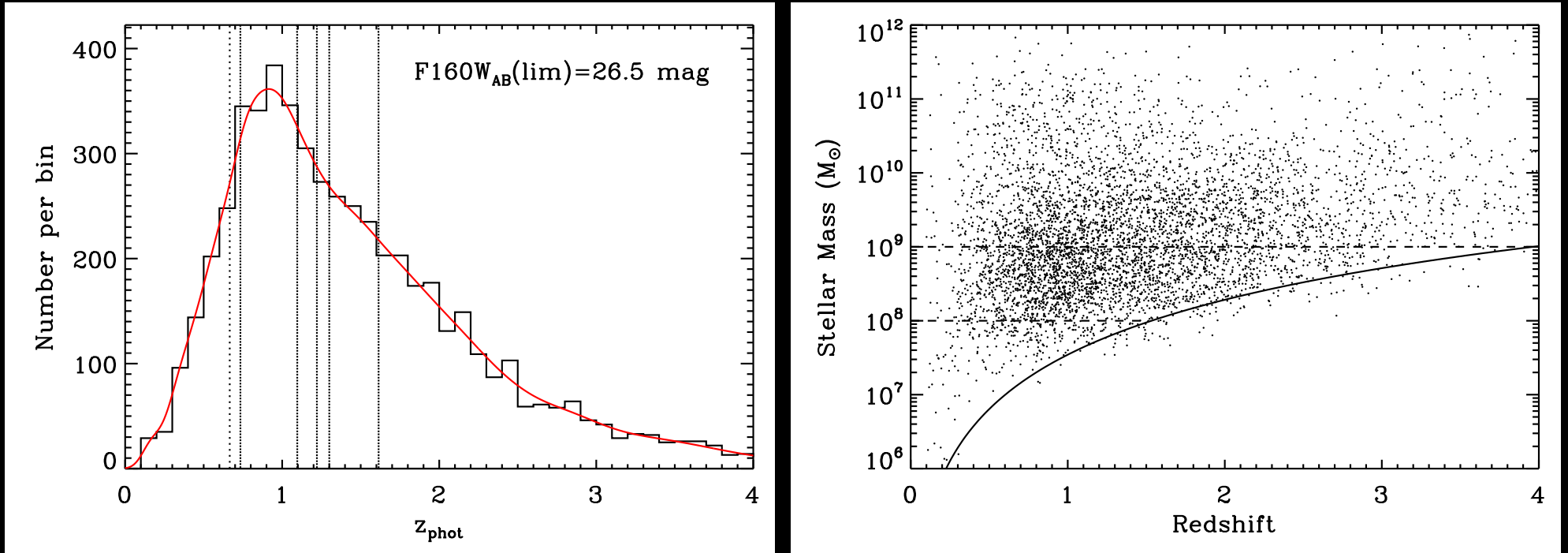


- Limited flux-range as yet, which limits the M^* , ϕ^* , α -accuracy.
- Deep wide-field WFC3 UV: UV LF's in z-range hard to do from ground.
- Deep wide-field WFC3 UV: significantly improves bright-end, M^* & ϕ^* .



Measured faint-end LF slope evolution (α ; top) and characteristic luminosity evolution (M^* ; bottom) from Hathi et al. 2010 (ApJ, 720, 1708).

- Still poorly determined LF parameters at $1 \lesssim z \lesssim 3$, when most stars born:
- Deep wide-field WFC3 UV imaging will vastly improve on this.



WFC3 ERS 10-band redshift estimates accurate to $\lesssim 4\%$ with small systematic errors (Hathi et al. 2010, 2012), resulting in a reliable $N(z)$:

- Measure masses of faint galaxies to AB=26.5 mag, tracing the process of galaxy assembly: downsizing, merging, (& weak AGN growth?).

ERS shows WFC3's new panchromatic capabilities on galaxies at $z \simeq 0-8$:

- Deep wide-field WFC3 UV will significantly improve SED-fits & photo-z's, both in rms and catastrophic failures (Cohen et al. 2012).